PHYSICAL REVIEW B **71**, 104205 (2005)

Chemical and electronic structures of liquid methanol from x-ray emission spectroscopy and density functional theory

Stepan Kashtanov,[1,2] Andreas Augustson,[3] Jan-Erik Rubensson,[3] Joseph Nordgren,[3] Hans Ågren,[1] Jing-Hua Guo,[2,*] and Yi Luo[1,†]

[1]*Theoretical Chemistry, Royal Institute of Technology, AlbaNova University Center, SE-10691, Stockholm, Sweden*
[2]*Advanced Light Source, Lawrence Berkeley National Laboratory, Berkeley, California 97720, USA*
[3]*Department of Physics, Uppsala University, Box 530, S-75121, Uppsala, Sweden*

(Received 2 November 2004; published 31 March 2005)

We have applied x-ray emission spectroscopy and density functional theory (DFT) to study the chemical and electronic structures of liquid methanol. The x-ray emission spectra at carbon and oxygen *K* edges of methanol in different hydrogen-bonded clusters are simulated. It is shown that hydrogen bonding strongly influences the spectral profile of O *K* emission, but not the C *K* emission. The methanol chain and ring conformations show a distinct difference in their electronic structures. The molecular orbitals of chains are strongly localized, whereas for the ring structures they show strong delocalization characteristics and behaviorlike covalent π orbitals in a conjugated system. A comparison of experimental spectra and DFT calculations suggests that liquid methanol comprises combinations of rings and chains of methanol molecules linked with hydrogen bonds and is dominated by structures with the size of six and eight molecules.

DOI: 10.1103/PhysRevB.71.104205 PACS number(s): 78.70.En, 79.90.+b, 82.30.Rs, 82.90.+j

I. INTRODUCTION

Liquid methanol has been widely studied due to its importance for technological and industrial applications. It is used in many ways (e.g., in direct fuel cells), providing a very promising and simple electrochemical converter.[1] It is also used as an organic solvent for investigation of protein-solvent reactions.[2] Methanol has unusual physical properties; it is stable over a wide range of temperatures, has a small viscosity coefficient (even smaller than liquid water), and an anomalous heat of vaporization.[3] It is also one of the simplest organic species for which hydrogen bonding is important in both its liquid and solid forms. Much experimental and theoretical work has therefore been devoted to understanding the electronic structure and the physical and chemical properties of liquid methanol.[4] A recent review can be found in Ref. 5.

The molecular geometry of liquid methanol has been the subject of much debate during the last 40 years. The complexity of its conformation in the liquid phase is a result of the peculiar dynamic behavior due to hydrogen bonding. In the crystal phase the methanol molecules are connected by hydrogen bonds to form one-dimensional chain structures.[6,7] Pauling argued from an energetic point of view that the molecules in liquid methanol form cyclic hexamer structures.[8] This hypothesis has both been supported and contested by various experimental and theoretical studies. It seems as though all simulations, ranging from classical molecular dynamics (MD),[9] Monte Carlo,[10] and *ab initio* molecular dynamics,[5,11–13] favor the existence of chain structures, although no consensus has been reached with respect to the average chain length. Neutron-diffraction results have led to different conclusions. A detailed analysis[14] based on earlier neutron diffraction[15,16] and x-ray scattering[17,18] indicated the presence of cyclic hexamers, thus confirming the early suggestion of Pauling. Simulations based on other neutron diffraction results,[19] however, point toward chains with up to ten molecules with an average of six. The latest Car-Parrinello *ab initio* molecular dynamics[13] simulations, on the other hand, indicate that the average chain length should be around ten methanol units.

The chain and ring structures of methanol molecules have a distinguishable electronic structure. The difference can be monitored by resonant soft x-ray emission (SXE) spectroscopy, which is sensitive to the local electronic structure of molecules. We have shown in our recent studies on liquid water that this technique can provide details about the changes in the electronic structure of water upon condensation, and thereby about the local hydrogen-bonding network of liquid water.[20,21] A double peak structure revealed in the SXE spectra of liquid methanol is found to be associated with the coexistence of chain and ring structures of methanol molecules with dominant sizes of six and eight.[22] Furthermore, the interaction between methanol and water in a methanol-water mixture has also been studied, and we have shown that the water molecules interact with methanol chains to form a ringlike structure. This finding sheds light on the microscopic origin of the anomalous entropy increase upon solution.[22] In the present work, we will provide the computational details and a comprehensive analysis of the electronic structures of methanol clusters in chain and ring forms. In addition, experimental spectra at the carbon *K* edge are presented and analyzed.

II. COMPUTATIONAL DETAILS

We combine *ab initio* Hartree-Fock and hybrid density-functional theory to study the geometrical and electronic structure, as well as the SXE spectra, of different methanol clusters (see Fig. 1). Geometry optimization and orbital analysis for rings and chains up to ten methanol units have been performed using Becke's three parameters hybrid [23] and

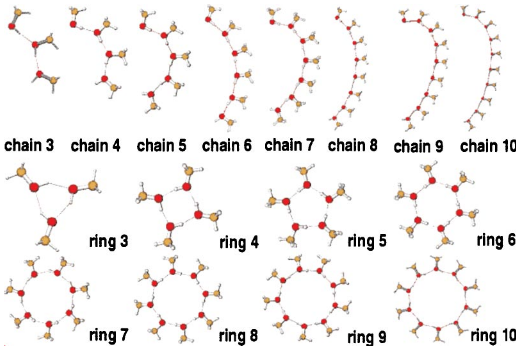

FIG. 1. (Color online) Optimized geometries of methanol ring and chain structures up to ten units.

Lee, Yang, and Par correlation[24] hybrid functional (B3LYP) with a 6-31G basis set in GAUSSIAN98 package.[25] The B3LYP functional has shown to be quite reliable for both structures and energies of different hydrogen-bonded clusters.[26–30] Calculations of the x-ray emission spectra were carried out at the Hartree-Fock level with the Sadlej basis set[31] using the DALTON program.[32] The use of Hartree-Fock allows us to include the long-range solvent effects by embedding the clusters in a dielectric medium, for which a spherical cavity with radii determined by the van der Waals radius of the outermost atoms is adopted. We have also found that the performance of Hartree-Fock for the spectral distribution is in good agreement with the B3LYP results. Both methods fall short in predicting the absolute transition energies at a sub-electron-volt range. For comparison with experimental results the calculated spectra are shifted uniformly. It should be stressed that the relative orbital energies are not affected by this shifting. The calculated spectra are convoluted with a Gaussian profile of linewidth 0.5 eV [the half-width at half maximum (HWHM)].

III. EXPERIMENT

The experiments were performed at beamline 7.0.1 at the Advanced Light Source, Lawrence Berkeley National Laboratory. The beamline comprises a 99-pole, 5 cm period undulator, and a spherical-grating monochromator covering the photon energy range between 80 and 1300 eV.[33]

The liquid samples were sealed in a cell and loaded into the experimental vacuum chamber for the liquid phase x-ray absorption spectroscopy (XAS) and x-ray emission spectroscopy (XES) measurements. The incident photon beam entered and exited from the same silicon nitride window of 1000 Å thickness. The base pressure of the experiment was 10×10^{-9} torr.

XAS spectra of liquid methanol were measured by using the x-ray-fluorescence-yield (FY) mode. The resolution of the monochromator was set to 0.2 eV for both the O 1*s* and C 1*s* absorption measurements. The XAS spectra were normalized by the photocurrent from a clean gold mesh in the photon beam to correct for intensity fluctuations of the photon beam. XES spectra were recorded using a high-resolution grating spectrometer.[34] The spectrometer was mounted parallel to the polarization vector of the incident photon beam. The resolution of spectrometer was set to 0.3 and 0.5 eV for C *K* and O *K* emission, respectively, and the excitation resolution from the monochromator was 0.3 and 0.5 eV for C *K* and O *K* edges, respectively.

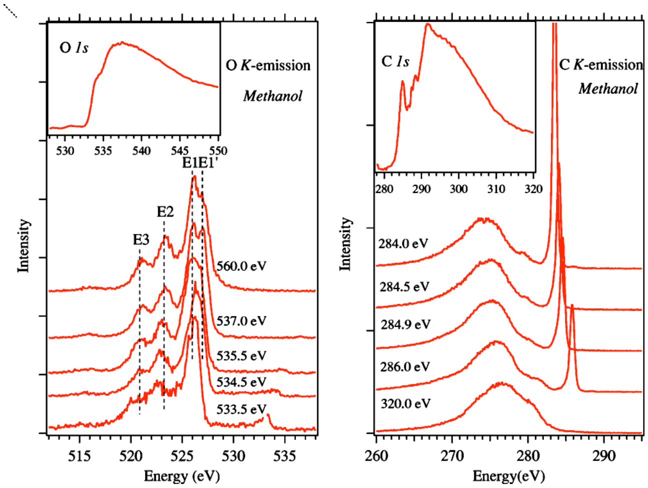

FIG. 2. Experimental resonant O 1*s* and C 1*s* x-ray emission spectra of pure methanol liquid. The insets in the figures show corresponding absorption spectra.

Figure 2 shows the O *K* and C *K* x-ray emission spectra of pure liquid methanol recorded at selected excitation energies. The O 1*s* and C 1*s* x-ray absorption spectra are displayed as the corresponding insets in Figs. 2(a) and 2(b). O 1*s* absorption of liquid methanol starts onset from 533 eV and shows a prepeak at 534.5 eV similar to that of liquid water.[20] The oxygen normal *K*-emission spectrum excited at 560 eV shows three emission bands: *E*1 (*E*1′), *E*2, and *E*3. The double- structure band *E*1 (*E*1′) exhibits dominant intensity and a strong dependence on the excitation energies. *E*1′ enhances at the excitation of 537 eV, while it nearly disappears at excitation below 534.5 eV. It indicates that the selective excitations enhance the contribution from one or another chemical specie. The carbon normal *K* emission excited 320 eV shows a broad emission band center at 276.5 eV with a shoulder at 280 eV. For the excitations near pre-edge, the shoulder is depressed and central emission band shifts in the line with the elastic peak due to the energy conservation in the resonant x-ray emission process.

IV. RESULTS

A. Methanol molecule

The methanol molecule belongs to the class of monatomic saturated alcohols with the common formula $C_nH_{2n+1}OH$ or usually written as *R*-OH, where *R* is a C_nH_{2n+1} alkyl radical. The oxygen atom in the hydroxyl group pulls the electron density over the OH bond, which makes this bond highly polarized with the negative charge localized on the oxygen atom and positive charge on the hydrogen atom, i.e., O^{d-}-H^{d+}. The polarization effect is reduced by the presence of alkyl radicals exhibiting a donor behavior. The flexibility of the hydrogen atom in structures, such as R-O^{d-}-H^{d+}, is less than that in water. The electronic structure of the metha-

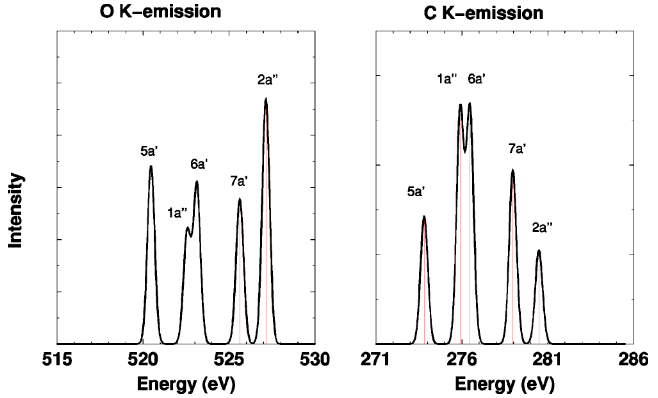

FIG. 3. Calculated oxygen and carbon x-ray *K*-emission spectra of methanol molecule in gas phase.

nol molecule in C_s symmetry can be expressed as $1a'^2 2a'^2 3a'^2 4a'^2 5a'^2 1a''^2 6a'^2 7a'^2 2a''^2$.

The calculated O 1*s* and C 1*s* x-ray emission spectra of the methanol molecule, presented in Fig. 3, are in good agreement with previous experimental[35] and theoretical[36] results. Both show five valence orbitals with intensive electronic transition, including three a' (5–7 a') and two a'' (1–2 a'') orbitals. It tells that the the *p* orbitals of the carbon and oxygen atoms are highly hybridized. The comparison between oxygen and carbon spectra provides information about the character of the orbitals. For instance, the highest occupied molecule orbital (HOMO) $2a''$ has the largest intensity in the oxygen spectrum, indicating that this orbital is mainly of oxygen *p* character. One can conclude that the $5a'$, $7a'$,and $2a''$ orbitals are more oxygenlike, whereas the $1a''$ and $6a'$ orbitals are more carbonlike.

Based on the orbital analysis, one can obtain quite detailed information about each orbital. One finds that the electron density of the $5a'$ orbital is oriented in the molecular plane defined by carbon, oxygen, and hydrogen of the H-C-O-H group. This orbital is extended over these atoms. The $1a''$ orbital has its electron density oriented perpendicularly to the H-C-O-H plane. It is a result of the interaction between the out of H-C-O-H plane *p* orbital of oxygen and the two out of the plane sp^3-hybridized C-H orbitals. The $6a'$ orbital is a mixture of two *p* orbitals from carbon and oxygen, and of the 1*s* orbital of the three hydrogen atoms in the $-CH_3$ group. Another *p* orbital of the oxygen atom and the *p* character of the in plane $-CH_3$ alkyl radical group give rise to the $7a'$ orbital. The HOMO, $2a''$, of the methanol molecule is constructed mainly by the out-of-the-plane *p* orbital of carbon and oxygen atoms. The electron density of this orbital has a tendency to be localized on the oxygen atom.

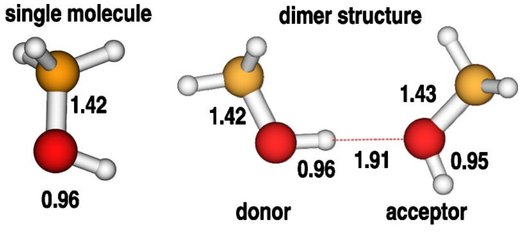

FIG. 4. (Color online) Optimized geometries of the single methanol molecule and its dimer.

B. Methanol dimer

Before calculating the more complex molecular clusters corresponding to liquid methanol, we investigate the methanol dimer to learn how hydrogen bonding affects the electronic structure. The result of geometry optimization using B3LYP is shown in Fig. 4. Our calculated bond lengths are in good agreement with results obtained from other methods, see Table I for a comparison. The oxygen-oxygen bond length $r_{\text{O-O}}$ and hydrogen-oxygen bond length $r_{\text{H-O}}$ are found to be 2.87 Å and 1.91 Å, respectively, from our calculations, which are in reasonable agreement with the experimental values of $r_{\text{O-O}}=2.98$ Å and $r_{\text{H-O}}=1.96$ Å.[38,39] The hydrogen bond length of the methanol dimer is slightly longer than that for the water dimer ($r_{\text{H-O}}=1.95$ Å),[21] suggesting that the hydrogen bonding effect on the methanol dimer is smaller than that of the water dimer.

The SXE spectra in Fig. 5 show the local molecular orbitals of the individual oxygen atoms (hydrogen-donor and hydrogen-acceptor) and the total contribution of the methanol dimer. The oxygen *K*-emission spectra from the individual methanol molecule show a similar spectral profile as the monomer apart from two additional weak features, which are marked *d*1 and *d*2 for the donor and *a*1 and *a*2 for the acceptor. The orbital character of the major spectral peaks of the dimer are, in general, the same for the monomer. The observation of these extra spectral features is a strong indication of orbital mixture, since x-ray emission is an element-specific technique and the spectrum of each oxygen atom should provide the information about the local *p* population

TABLE I. Optimized bond lengths and angles for the methanol dimer from different methods.

Method	C-O	O-H	O-O	$\angle(C\text{-}O\text{-}H)$	$\angle(O\cdots H\text{-}O)$
B3LYP[a]	1.43(1.42)	0.95(0.96)	2.87	114.2°(113.6°)	177.9°
BLYP[b]	1.46(1.45)	0.98(0.99)	2.94		173.4°
BLYP[c]	1.45(1.43)	0.97(0.98)	2.92		171.5°
MP2[d]	1.43(1.42)	0.96(0.97)	2.88	109.6°(108.8)°	177.4°

[a] This work.
[b] CPMD Ref. 11.
[c] ADF Ref. 11.
[d] Reference 37.

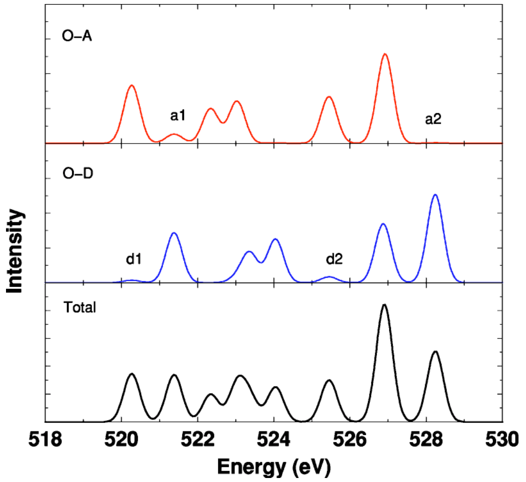

FIG. 5. Calculated oxygen *K*-emission spectra of the methanol dimer. Letters *D* and *A* indicate donor and acceptor oxygen sides, respectively. The features resulting from orbital mixing are labeled as *d*1, *d*2 and *a*1, *a*2.

of the oxygen that is measured. The electron sharing takes place at the orbitals involving the O-H bond. Like the gas phase water dimer, the electron sharing between two molecules is quite weak. We have shown in our previous study on liquid water[21] that the covalent feature of the hydrogen bonding can hardly be observed in the gas phase but should be detectable in the liquid phase. This is because the mutual orientation of water molecules in the liquid phase is very different from that in the gas phase. Depending on the mutual positioning of water molecules, orbital mixing can involve different orbitals and be very strong. The reliability of using interaction potentials generated from the gas-phase dimer in the molecular dynamics simulation was questioned in Ref. 21.

The interaction between methanol molecules in the dimer is dominated by the pure electrostatic interaction. This is best illustrated by the typical push-pull behavior that results in the relative shift of the spectra (~1 eV) from the donor and the acceptor. The total contribution from both oxygen atoms appears to give a very broad spectral profile.

C. Methanol chains

It seems that almost all dynamics studies find that liquid methanol consists of chain structures,[5,9–13] although there is no consensus about the average size of the chain. This is probably because that most interaction potentials are based on the methanol dimer model. As we have shown in the previous section, the methanol dimer is strongly polarized.

We have chosen a chain with six methanol units (chain6) as a model to analyze the hydrogen bonding effects on the electronic structures of methanol in chain structures. In general the methanol long chain can be represented as an extended dimer model. The optimized structure of chain6 and its emission spectra are given in Fig. 6.

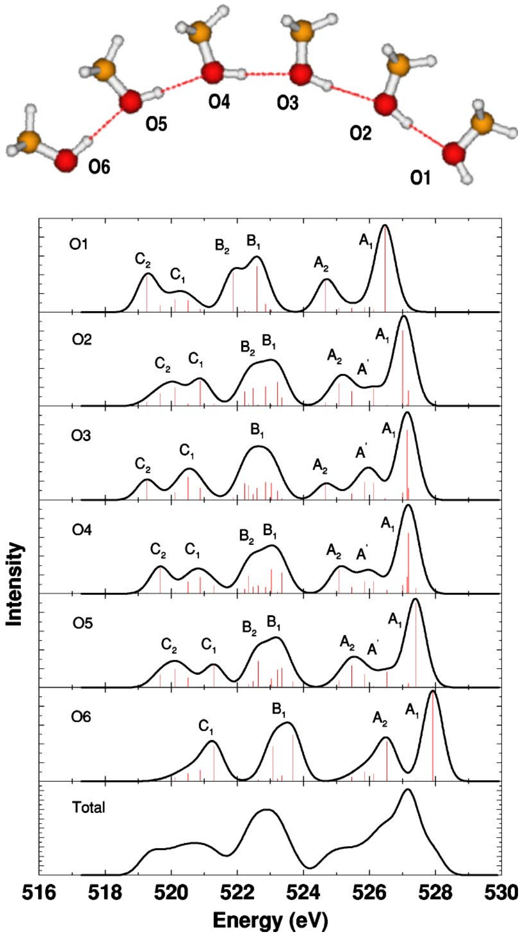

FIG. 6. (Color online) Optimized structure and calculated O *K* emission of chain with six methanol units. The labels of oxygen atoms correspond to the labels on emission spectra.

The chain of methanol molecules does not form a straight line because of the steric effect. The emission spectra of individual oxygen atoms and their summation are shown in Fig. 6. In this system, the two end oxygen atoms, O1 and O6, act only as hydrogen acceptor and hydrogen donor, respectively, whereas other oxygen atoms in the middle are capable of giving (donor) and receiving (acceptor) hydrogen. With the help of the dimer spectra, it is easy to understand the energy shifting among spectra of the individual oxygen at-

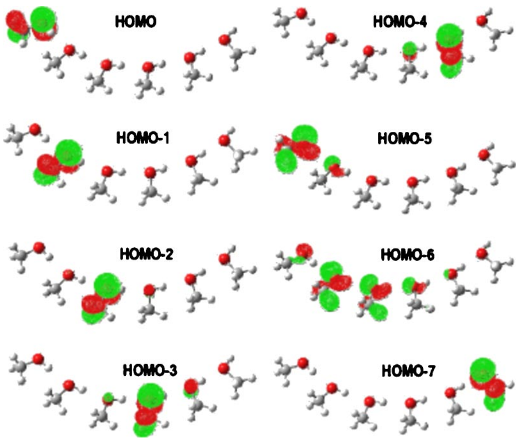

FIG. 7. (Color online) Highest occupied molecular orbitals of chain with six methanol units.

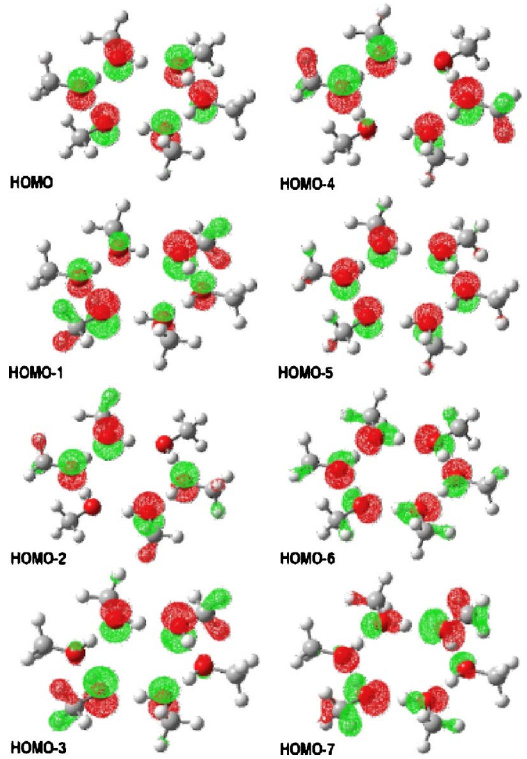

FIG. 8. (Color online) The eight highest occupied molecular orbitals of ring with six methanol units.

oms. It is noted that the energy shift between spectra of O6 and O1 is close to 1.5 eV, larger than that for the dimer. This is a result of the cooperative effect of the hydrogen bonding, i.e., the interaction gets stronger with more hydrogen bonds involved. With respect to the spectrum of O6 (the donor case), all other spectra shift down in energy, i.e., showing a net pushing effect. It thus implies that there is an imbalance between the push and pull forces acting on the oxygen atoms in the middle. The whole system is strongly polarized.

The emission spectra show basically three strong spectral features, which are labeled *A*, *B*, and *C*. The O6 spectrum resembles the spectrum of the monomer quite well. Strong orbital mixing is observed in the spectra of the middle molecules. The most noticeable sign of the orbital mixture is the change of the spectral profile A' and the broadening of the spectral feature *C*. It is important to know that the orbital mixture among different methanol molecules is introduced by the hydrogen donor.

The eight highest occupied molecular orbitals, HOMO, HOMO-1,…, HOMO-7, of the chain6 cluster is presented in Fig. 7. All orbitals, except HOMO-6, show strong localization character, which is moving toward the acceptor side of the chain structure with decreasing orbital energy. Orbital mixing can be found in HOMO-6 between two neighboring methanol molecules.

D. Methanol rings

In methanol ring structures, each oxygen atom possesses two hydrogen bonds, one acceptor and one donor. The competition between the push and pull forces should result in an electronic structure that is largely different from that of the chain structures. Indeed, a distinct difference between ring of six methanol units (ring6) and chain6 in molecular orbitals has been found. The eight highest occupied molecular orbitals of ring6 are shown in Fig. 8. In contrast to the case of the chain, all orbitals in ring6 are fully delocalized. The electron distribution in the ring structure seems to resemble the benzene ring very well. We recall that the electron delocalization in a benzene ring, or conjugated systems in general, is a result of strong covalent bonds, whereas in the case of methanol rings the driving force is a hydrogen bond, which is normally considered to be weak with electrostatic nature. Probably the methanol rings are the best examples to illustrate the covalent contribution to the hydrogen bond. Such a close high-symmetry species often has lower energy than isomers of lower symmetry. The total energy calculation clearly shows that the six-ring is lower in energy than the six-chain. Although the gas-phase energy value is not di-

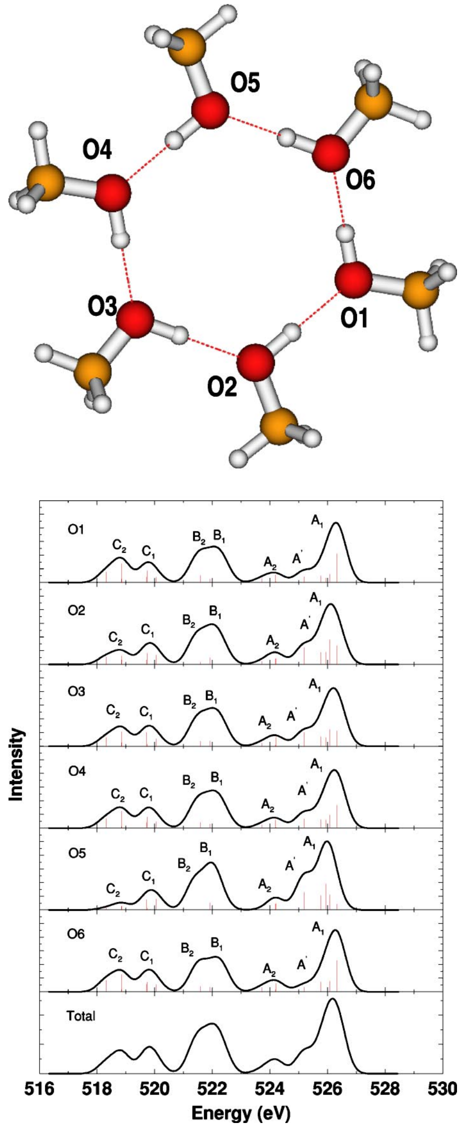

FIG. 9. (Color online) Optimized structure and calculated O *K* emission of ring with six methanol units. The labels of oxygen atoms correspond to the labels on the emission spectra.

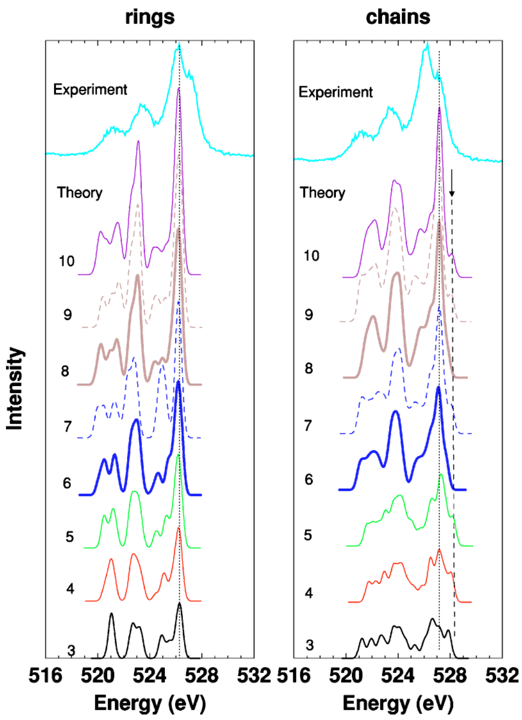

FIG. 10. (Color online) Calculated oxygen *K*-emission spectra of ring and chain structures of methanol and comparison with experiment. Experimental *K*-emission spectrum measured at 320 eV excitation energy. Amount of methanol molecules in ring and chain structures used for theoretical simulations is shown by numbers at corresponding spectral curve.

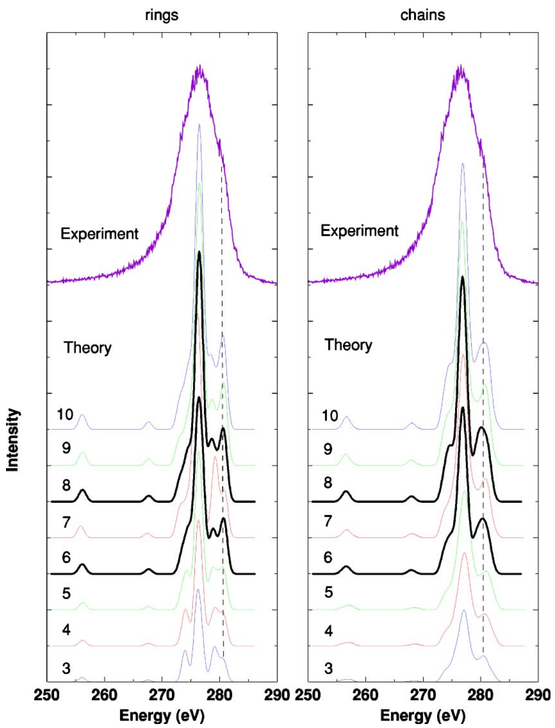

FIG. 11. (Color online) Calculated carbon *K*-emission spectra of ring and chain structures, and comparison to experiment. Experimental *K*-emission spectrum measured at 320 eV excitation energy. Amount of methanol molecules in ring and chain structures used for theoretical simulations is shown by numbers at corresponding spectral curve.

rectly relevant to that of the liquid phase, one still should expect predictions of ring structures in dynamics simulations. The absence of such predictions suggests that the existing dynamics simulation models are not capable of describing the strong covalent character of the rings.

Optimized structure and O *K* emission spectra of the six-ring are presented in Fig. 9. As expected from the orbital picture, spectra from individual oxygen atoms are almost identical. A very small difference among spectra can be found, which is because the 6-ring does not have a perfect symmetry and the hydrogen bond length is slightly different for different pairs of methanol molecules. It is noted that the distance between neighboring oxygen atoms is ~2.80–2.88 Å in the six-ring, and 2.88–3.01 Å in the six-chain. The slightly shorter O-O bond distance in the six-ring results in a stronger intermolecular interaction and is associated with stronger orbital mixing. In comparison to the spectrum of the monomer, one finds that the spectra of the six-ring are much broader because of the strong delocalization and orbital mixing. It is noted that the unoccupied molecular orbitals of six-chains and six-rings have the same feature as the corresponding occupied orbitals, localized for chains and delocalized for rings.

E. Liquid methanol

One finds that the total spectra of chain6 and ring6 have a relative energy shift of ~1 eV, which should be well resolved with the current experimental resolution. We have calculated the emission spectra of several ring and chain structures, ranging from three to ten units. The results together with the experimental emission spectrum are shown in Fig. 10. The most striking observation is the double peak structure of the outermost experimental spectral band, which can be assigned to contributions from chains and rings. It leads directly to the conclusion that the liquid methanol consists of a mixture of ring and chain structures. The results obtained from early studies are thus partially correct.

The emission peak at 526.2 eV in the experimental spectrum corresponds to the ring structures, and the peak at 527.2 eV is due to emission from the chain structures. It is noted that the 1 eV separation between the double peaks is well reproduced by the calculations. The spectra of ring structures seem to be insensitive to the size of the system. A peculiar behavior can be found for the case of rings. For the short chains, such as chain3 to chain5, the spectral bands are very broad. This can be understood because in these cases, each oxygen atom has its unique surrounding and, therefore, well-separated spectrum. When the chain gets longer, the middle oxygen atoms become more identical and the total spectrum becomes sharper. The long chain structures can be further discriminated by a small shoulder above the maximum of the outermost band. This shoulder has contribution from the hydrogen donor methanol at the end of the chain, like O6 in the six-ring structure. The energy separation between this shoulder and the maximum of the band strongly depends on the size of the clusters. It is interesting to see that due to small separation, such a shoulder does not appear in the spectra of the six-rings and eight-rings. By inspecting the experimental spectrum, there is no clear shoulder structure at the high-energy side of the outermost spectral band. It, thus, suggests that the most possible chain structures in liquid methanol should consist of six and eight units. The fact that the double peaks have almost the same intensity allows one to determine the size of the ring structures in liquid methanol, which should be same as the chains, i.e. methanol rings with six and eight units.

We have also computed the C *K* emission of all ring and chain structures. As one can see from Fig. 11, it is difficult to select out any particular structures by comparing the calculations and experiment. Nevertheless, two spectral structures located at 274 eV and 280 eV are well reproduced by the calculations. It is noted that the summation of C *K* emission spectra of rings and chains with six and eight units compare well with the experiment.

V. SUMMARY

We have demonstrated the power of x-ray emission spectroscopy for determining electronic and geometrical structures of liquids. With the help of theoretical analysis, information on the structure of liquid methanol has been revealed in this study. It is unambiguously shown that liquid methanol is a mixture of ring and chain structures, dominated by six and eight methanol units. The molecular orbitals of the ring structure with six methanol units show striking similarity to those of the benzene ring, which indicates that the hydrogen bonding in the ring structures have significant covalent contributions. It is noted that the electronic structure of the methanol dimer is as polarized as the other chain structures, but that it is completely different from the rings. This is probably the reason that molecular dynamics based on the potentials derived from the methanol dimer does not predict ring structures. Potentials that take into account the unique covalent contribution to hydrogen bonding in ring structures need to be constructed for future molecular dynamics simulations.

ACKNOWLEDGMENTS

This work was supported by the Swedish Research Council (VR), the Carl Trygger Foundation (CTS), the Göran Gustafson Foundation for Research in Natural Science and Medicine, and National Supercomputer Center (NSC) in Linköping, Sweden. The experimental work at ALS, Lawrence Berkeley National Laboratory was supported by U.S. Department of Energy, under Contract No. DE-AC03-76SF00098.

---

*Corresponding author. Electronic address: jguo@lbl.gov

†Corresponding author. Electronic address: luo@theochem.kth.se

[1] S. Mukerjee and R. C. Urian, Electrochim. Acta **47**, 3219 (2002).

[2] W. R. Cannon and S. J. Benkovic, J. Biol. Chem. **273**, 26257 (1998).

[3] Kevin R. Wilson, R. D. Schaller, D. T. Co, R. J. Saykally, Bruce S. Rude, T. Catalano, and J. D. Bozek, J. Chem. Phys. **117**, 7738 (2002).

[4] B. M. Ladanyi and M. S. Skaf, Annu. Rev. Phys. Chem. **44**, 335 (1993).

[5] E. Tsuchida, Y. Kanada, and M. Tsukada, Chem. Phys. Lett. **311**, 236 (1999).

[6] B. H. Torrie and S.-X. Weng, Mol. Phys. **67**, 575 (1989).

[7] K. J. Tauer and W. N. Lipscomb, Acta Crystallogr. **5**, 606 (1952).

[8] L. Pauling, *The Nature of Chemical Bond*, 3rd ed. (Oxford University, Oxford, 1967).

[9] M. Haughney, M. Ferrario, and I. R. McDonald, J. Phys. Chem. **91**, 4934 (1987).

[10] W. L. Jorgensen, J. Am. Chem. Soc. **103**, 134 (1981).

[11] J.-W. Handgraaf, T. S. van Erp, and E. J. Meijer, Chem. Phys. Lett. **367**, 617 (2003).

[12] J. A. Morrone and M. E. Tuckerman, J. Chem. Phys. **117**, 4403 (2002).

[13] M. Pagliai, G. Cardini, R. Righini, and V. Schettino, J. Chem. Phys. **119**, 6655 (2003).

[14] S. Sarkar and R. N. Joarder, J. Chem. Phys. **99**, 2032 (1993).

[15] D. G. Montague, I. P. Gibson, and J. C. Dore, Mol. Phys. **44**, 1355 (1981).

[16] Y. Tanaka, N. Phtomo, and K. Arakawa, Bull. Chem. Soc. Jpn. **58**, 644 (1984).

[17] A. H. Narten and A. Habenschuss, J. Chem. Phys. **80**, 3387 (1984).

[18] M. Magini, G. Paschina, and G. Piccaluga, J. Chem. Phys. **77**, 2051 (1982).

[19] T. Yamaguchi, K. Hidaka, and A. K. Soper, Mol. Phys. **96**, 1159, (1999); **97**, 603 (1999).

[20] J.-H. Guo, Y. Luo, A. Augustsson, J.-E. Rubensson, C. Såthe, H. Ågren, H. Siegbahn, and J. Nordgren, Phys. Rev. Lett. **89**, 137402 (2002).

[21] S. Kashtanov, A. Augustsson, Y. Luo, J.-H. Guo, C. Såthe, J.-E. Rubensson, H. Siegbahn, J. Nordgren, and H. Ågren, Phys. Rev. B **69**, 024201 (2004).

[22] J.-H. Guo, Y. Luo, A. Augustsson, S. Kashtanov, J.-E. Rubensson, D. Shuh, H. Ågren, and J. Nordgren, Phys. Rev. Lett. **91**, 157401 (2003).

[23] A. D. Becke, Phys. Rev. A **38**, 3098 (1988).

[24] C. Lee, W. Yang, and R. G. Parr, Phys. Rev. B **37**, 785 (1988).

[25] M. J. Frisch, G. W. Trucks, H. B. Schlegel, G. E. Scuseria, M. A. Robb, J. R. Cheeseman, V. G. Zakrzewski, J. A. Montgomery, Jr., R. E. Stratmann, J. C. Burant, S. Dapprich, J. M. Millan, A. D. Daniels, K. N. Kudin, M. C. Strain, O. Farkas, J. Tomasi, V. Barone, M. Cossi, R. Cammi, B. Mennucci, C. Pomelli, C. Adamo, S. Clifford, J. Ochterski, G. A. Petersson, P. Y. Ayala, Q. Cui, K. Morokuma, D. K. Malick, A. D. Rabuck, K. Raghavachari, J. B. Foresman, J. Cioslowski, J. V. Ortiz, B. B. Stefanov, G. Liu, A. Liashenko, P. Piskorz, I. Komaromi, R. Gomperts, R. L. Martin, D. J. Fox, T. Keith, M. A. Al-Laham, C. Y. Peng, A. Nanayakkara, C. Gonzalez, M. Challacombe, P. M. W.

Gill, B. Johnson, W. Chen, M. W. Wong, J. L. Andres, M. Head-Gordon, E. S. Replogle, and J. A. Pople, GAUSSIAN98, Gaussian Inc., Pittsburgh, 1998.

[26] S. Suhai, J. Phys. Chem. **99**, 1172 (1995).

[27] J. E. Del Bene, W. B. Person, and K. Szczepaniak, J. Phys. Chem. **99**, 10705 (1995).

[28] J. J. Novoa and C. Sosa, J. Phys. Chem. **99**, 15837 (1995).

[29] P. Süle and A. Nagy, J. Chem. Phys. **104**, 8524 (1996).

[30] L. Gonsález, O. Mó, and M. Yáñez, J. Comput. Chem. **18**, 1124 (1997).

[31] A. J. Sadlej, Theor. Chim. Acta **79**, 123 (1991).

[32] T. Helgaker, H. J. Aa. Jensen, P. Jrgensen, J. Olsen, K. Ruud, H. Ågren, A. A. Auer, K. L. Bak, V. Bakken, O. Christiansen, S. Coriani, P. Dahle, E. K. Dalskov, T. Enevoldsen, B. Fernandez, C. Httig, K. Hald, A. Halkier, H. Heiberg, H. Hettema, D. Jonsson, S. Kirpekar, R. Kobayashi, H. Koch, K. V. Mikkelsen, P. Norman, M. J. Packer, T. B. Pedersen, T. A. Ruden, A. Sanchez, T. Saue, S. P. A. Sauer, B. Schimmelpfennig, K. O. Sylvester-Hvid, P. R. Taylor, and O. Vahtras, *Dalton, A Molecular Electronic Structure Program, Release 1.2* (Dalton, 2001); see http://www.kjemi.uio.no/software/dalton/dalton.html

[33] T. Warwick, P. Heimann, D. Mossessian, W. McKinney, and H. Padmore, Rev. Sci. Instrum. **66**, 2037 (1995).

[34] J. Nordgren, G. Bray, S. Cramm, R. Nyholm, J. E. Rubensson, and N. Wassdahl, Rev. Sci. Instrum. **60**, 1690 (1989).

[35] J.-E. Rubensson, N. Wassdahl, R. Brammer, and J. Nordgren, J. Electron Spectrosc. Relat. Phenom. **47**, 131 (1988).

[36] H. Ågren and A. Flores-Riveros, J. Electron Spectrosc. Relat. Phenom. **56**, 259 (1991).

[37] O. Mó, M. Yáñez and J. Elguero, J. Chem. Phys. **107**, 3592 (1997).

[38] F. J. Lovas, S. P. Belov, M. Y. Tretyakov, W. Stahl, and R. D. Suenram, J. Mol. Spectrosc. **170**, 478 (1995).

[39] F. J. Lovas and H. Hartwig, J. Mol. Spectrosc. **185**, 98 (1997).